

FAST RELEASE OF NUCLEAR REACTION PRODUCTS FROM REFRACTORY MATRICES

L.C. Carraz, I.R. Haldorsen<sup>\*)</sup>, H.L. Ravn,  
M. Skarestad<sup>\*)</sup> and L. Westgaard<sup>\*)</sup>

The ISOLDE Collaboration

CERN, Geneva, Switzerland

ABSTRACT

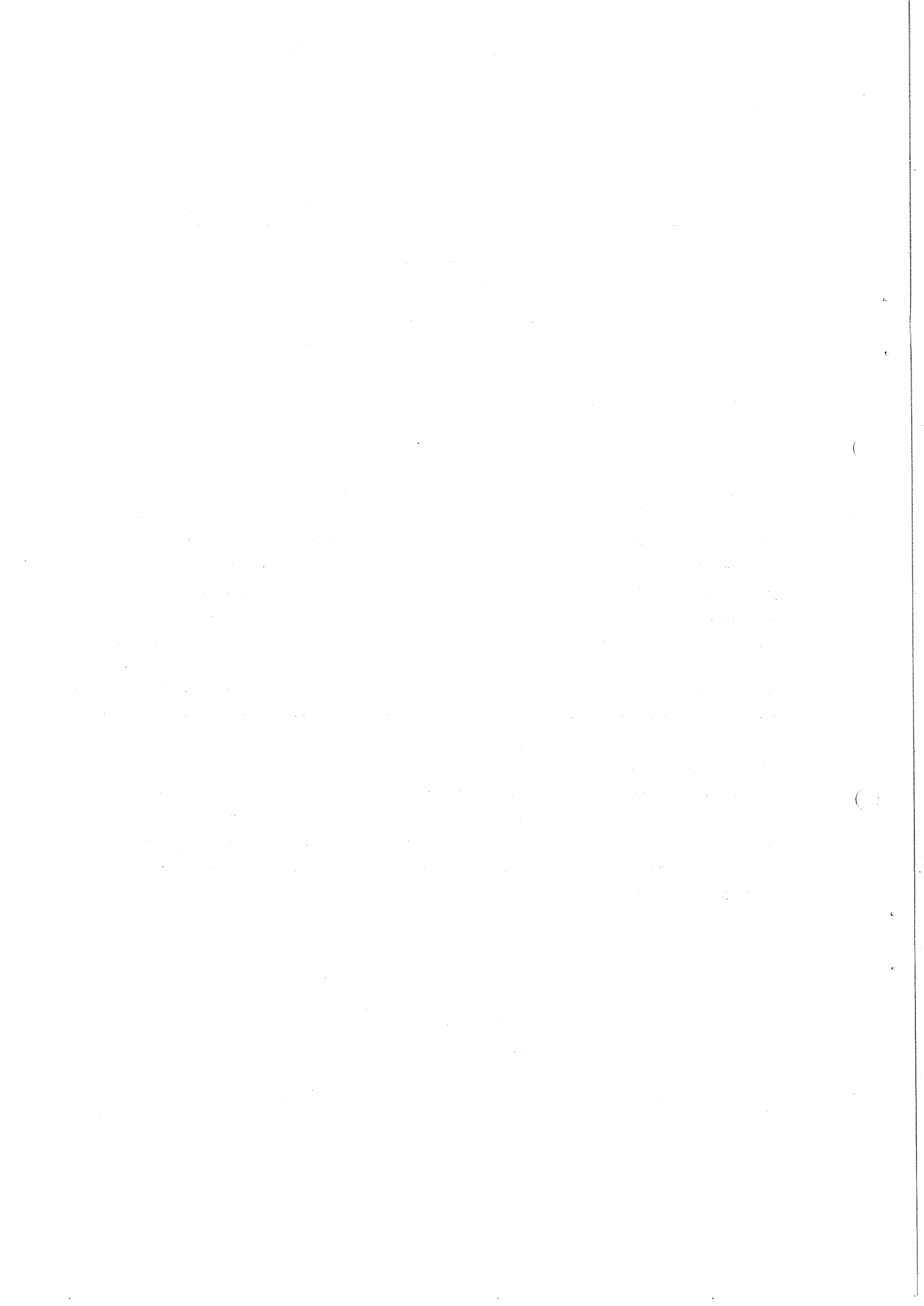
Release rates of various reaction products formed by 600 MeV proton irradiation in samples of W, Ta, Hf, Mo, Nb, V, UC, VC, TiC, BaB<sub>6</sub>, CeB<sub>6</sub>, BaZrO<sub>3</sub>, CeS, Ce<sub>3</sub>S<sub>4</sub> and uranium-impregnated graphite cloth (20 μm fibres) have been measured. The samples, in the form of powders (~ 10 μm particles), fibre cloth, or in one case liquid (Ce<sub>3</sub>S<sub>4</sub>), were contained in Ta or graphite at temperatures in the neighbourhood of 2000°C. At such high temperatures, fast release was observed for a number of elements, i.e. S, Cl, Ar, K, Ca, Se, Rb, Sr, Ag, Cd, In, Sn, Sb, Te, I, Xe, Cs, Ba, Yb. The release data are accounted for by different diffusion and desorption processes, allowing each system to be characterized by a temperature-dependent parameter μ, related to physical quantities like activation energy, diffusion coefficient, and particle dimension. On this basis, the different matrices are compared in terms of expected delay properties for on-line application. By taking into account material density, vapour pressure, and stability towards sintering we indicate some promising target systems for on-line application at the ISOLDE isotope separator, coupled on-line with the CERN 600 MeV Synchrocyclotron. Some 30 different product elements are expected to be separated from these target systems.

Geneva - 3 August 1977

(Submitted to Nuclear Instrum. Methods)

---

<sup>\*)</sup> Present address: Chemical Institute, University of Oslo, Blindern, Oslo, Norway.



## 1. INTRODUCTION

The purpose of the ISOLDE on-line isotope separator<sup>1-3)</sup> at the CERN Synchro-cyclotron is to provide mass-separated sources of short-lived isotopes of as many different elements as possible, in order to allow systematic studies of the properties of nuclei far removed from beta stability. An essential part of the facility is the target system, where a broad range of nuclides are formed as end products in complex reactions between the impinging 600 MeV protons and the target nuclei. A great effort has been put into the development of target and ion-source systems, which should combine high production yields with short hold-up times between the formation of the desired product in the target and its subsequent mass separation and collection for measurement. An account of this work up to 1974, including a complete list of earlier references, may be found in the paper by Ravn et al.<sup>4)</sup>.

The penetrating power of the 600 MeV protons demands the use of thick targets in order to make efficient use of the primary beam, and the time-limiting step in the whole process of on-line mass separation is then generally found to be the (continuous) transfer of the reaction products from the target matrix and out into the free volume above the target. One way of reducing the delay in this process is to use liquid targets, and a popular target type at ISOLDE has been molten metals at temperatures up to 1500°C, where the release of volatile products apparently is governed by the rate of desorption from the liquid surface<sup>4,5)</sup>.

The early use of refractory target compounds by Klapisch et al.<sup>6)</sup> and Hansen et al.<sup>7)</sup> prompted a systematic investigation of long-term chemical and physical stability, as well as release rates of selected tracer elements, for a number of refractory materials, in order to evaluate their possible utility as ISOLDE targets. Preliminary data from this study have been reported<sup>3)</sup> at a recent conference. The most spectacular application has so far been the observation<sup>8)</sup> of the new Rb isotope, the  $I^{\pi} = 0^{+}$  self-conjugate nuclide  ${}_{37}^{74}\text{Rb}$  of half-life 64.9 msec, produced from a niobium-powder target at 2200°C.

We discuss in Section 2 the basic principles for choosing refractory target materials and list some characteristic properties of the materials taken for investigation in the present study.

After describing in Section 3 the experimental techniques, we give in Section 4 the results of a search for suitable containers as well as release-rate data.

In Section 5 we treat the release-rate results in the framework of a simple diffusion model and discuss in detail the behaviour of the individual systems in view of their prospective use as on-line targets.

Section 6 contains some additional comments on the relevance of the present investigation for future on-line application.

## 2. CHOICE OF MATERIALS

The idea behind the use of refractory powders as target material is to combine short solid-diffusion paths and high temperature in order to ensure fast release of volatile reaction products. In general, the temperature should be as high as possible in order to enhance diffusion and desorption processes, without exceeding the melting points of the powders or producing intolerable pressure increases. In Table 1, columns 2-4, are summarized some physical and thermodynamic properties<sup>9-15)</sup> of the investigated materials. From these data we have estimated some maximum temperatures (Table 1, column 6) at which the systems can be operated, assuming that in order to assure proper operation of the ion source, a vapour pressure of less than  $10^{-3}$  Torr must be required<sup>4)</sup>.

In general, we notice that the metal powders are sufficiently stable to be run at temperatures above 2000°C, while refractory compounds of borides, sulfides, oxides, and most carbides, are limited to temperatures slightly below 2000°C.

The optimum target thickness, i.e. of one interaction length for the 600 MeV protons, corresponds to  $\sim 45$  g/cm<sup>2</sup> for V and  $\sim 160$  g/cm<sup>2</sup> for U, taken as extreme examples of prospective target materials discussed in this paper. Assuming about 50% porosity of the powdery material, it is seen from the densities quoted in Table 1 that a 20 cm long container (our practical limit for mechanical design) fulfils this requirement in most cases.

The release rates of various products formed upon irradiation of the powders are closely related to their diffusion coefficients in the solid particles. A rough estimate of the lower limit of these coefficients is often obtained by looking at the self diffusivities<sup>16)</sup>, and in Table 1, column 5, we have included some data of this kind. Note that, in general, the activation energy for self diffusion in metals is related to quantities reflecting the strength of atomic binding. A useful empirical relationship has been pointed out by LeClaire<sup>17)</sup>:

$$Q \sim 38 \times T_m,$$

where  $Q$  is the activation energy (cal/mol) and  $T_m$  is the melting point of the metal in °K.

The transport of substitutional impurities in metals is usually controlled by vacancy mechanisms. In such cases one can expect the impurity diffusion coefficients to take values about a factor 10-20 higher than the corresponding self-diffusion coefficients<sup>16)</sup>. However, in certain cases, when interstitial

mechanisms dominate, orders of magnitude in favour of impurity diffusion can be experienced<sup>16)</sup>. Strong components of this mechanism often appear in metals with bcc crystal structure, a structure which is exhibited by all metals included in Table 1.

### 3. EXPERIMENTAL TECHNIQUES

#### 3.1 Vacuum oven

The preparations and release studies described below were performed in an oven mounted inside the vacuum chamber ( $5 \times 10^{-5}$  Torr) of a standard evaporation unit, as shown in Fig. 1. The oven, which consists of a tantalum tube mounted between two water-cooled current feedthroughs, could be heated to a maximum temperature of 2200°C. The temperatures were measured by means of a two-colour optical pyrometer with an accuracy of  $\pm 10^\circ\text{C}$  around 2000°C.

#### 3.2 Preparation of samples

The physical form and origin of the initial materials follow from Table 2.

In most cases the samples were prepared by heating (sintering) of about 5 g of the powder in a suitable container (tantalum or graphite, see Table 1, column 7) at a temperature between 1800-2000°C for 5-15 min in the vacuum oven.

A different procedure was used in the preparation of uranium-impregnated graphite cloth, where the method<sup>18)</sup> developed at OSIRIS was applied, with the addition of one more heating step. After decomposition of  $\text{UO}_2(\text{NO}_3)_2$  at 900°C the samples were heated to 1700°C in vacuum for about 3 h, in order to transform the initially formed uranium oxides completely into UC. By examination under a microscope no deposit was visible on the cloth fibres, indicating that the UC had formed a solid solution in the graphite. The amount of uranium in the final samples averaged about 30-40 mg/cm<sup>2</sup> cloth.

$\text{Ce}_3\text{S}_4$  ("cerium black") was prepared by vacuum heating of  $\text{Ce}_2\text{S}_3$  at 2000°C for 1 h<sup>13)</sup>.

#### 3.3 Test of crucibles

All the materials listed in Table 2 have been tested in quantities of about 5 g in boats made of Ta over prolonged periods of heating at temperatures around 2000°C. Those which were found to attack the Ta container were subsequently tested in graphite crucibles under the same conditions.

During these tests some measurements of evaporation losses were included by weighing the samples before and after heating.

### 3.4 Irradiations and release measurements

Samples were irradiated with 600 MeV protons in the external beam of the Synchro-cyclotron for periods of 1 hour to several days. Following a cooling period depending upon the half-life of the nuclide(s) to be measured, it was possible to identify a number of specific spallation/fission products in the samples by means of  $\gamma$ -ray spectroscopy, using a large-volume Ge(Li) detector. The  $\gamma$ -rays assigned to radio-nuclides used for the release measurements are listed in Table 3.

The release measurements were performed by placing a sample (typically about 100 mg and less than 1  $\mu$ Ci activity) in the oven. Temperature equilibrium between the tube and sample was assumed to take place within a short time (less than 1 min). A  $\gamma$ -spectrum of the sample was recorded before and after a period of heating, and in most cases the heating and measurement cycle was repeated 1-3 times at each temperature. A new sample was taken for each new temperature. Since the release of products from  $Ce_3S_4$  was measured from molten samples, a slightly different method was used in this case. After irradiation a small sample was transferred to a tantalum evaporation boat, with a ratio of volume to surface area of 0.24 cm, and mixed with 1 g of inactive  $Ce_3S_4$ . The whole sample was kept molten in periods of  $\frac{1}{2}$  min, and  $\gamma$ -spectra were recorded between each period of heating.

## 4. RESULTS

### 4.1 Containment

Tantalum containers are in most cases found suitable for containment of the refractory metals up to their melting points. Hafnium can be kept in Ta only up to 2100°C, due to the formation of a low-melting alloy. The carbides and borides all caused serious corrosion in Ta within one hour at temperatures around 2000°C. On the other hand, graphite containers were found not to react with these compounds. For example, in a 48 hour test with UC, contained in graphite at 2000°C, no sign of corrosion could be seen.

According to Eastman et al.<sup>13)</sup> the cerium sulphides do not react with Mo crucibles, even in the molten forms. We found the same to be true for Ta.

Our final choice for crucible materials follows from Table 1, column 7.

### 4.2 Release rates

The results of release measurements in different matrices are shown as data points in Figs. 2-6, where the "fractional activity" of a number of elements is given as a function of sample heating time. The fractional activity of a given element is defined as the ratio between the activity of a characteristic isotope

in the sample after a heating period and the activity before any heating treatment. Some additional data, not included in the figures, are given in Table 4.

## 5. DISCUSSION

### 5.1 Release mechanisms

In order to understand the observed release properties and to make a quantitative comparison between different systems, we have to account for the release mechanisms that are in operation in such materials.

In powders, two different mechanisms are involved:

- i) The diffusion of the products to the surface of the powder particles.
- ii) The diffusion through the pores of the powder bed to the sample surface.

The relative importance of these processes depends on the particle dimensions and pore structure, as well as the physical and chemical properties of product elements. Our main concern will be those cases where mechanism (i) is found to be time controlling. Cases where (ii) is dominant are of less practical value, since the products belonging to this class in general will be strongly delayed in the multigram quantities of material needed for thick-target on-line experiments. In the following we will start by assuming process (i) to be time controlling and then discuss for which classes of products this assumption can be expected to be valid.

The diffusion in solids is described by Fick's second diffusion equation. By solving it for uniform spherical particles with an initially homogeneous activity distribution as boundary condition, the following expression for fractional activity  $F(t)$  can be derived<sup>19)</sup>:

$$F(t) = \frac{6}{\pi^2} \sum_{k=1}^{\infty} \frac{1}{k^2} e^{-k^2 \mu_s t}, \quad (1)$$

where  $t$  is the heating time and  $\mu_s$  is a diffusion parameter. In the practical case the particles are neither spherical nor of uniform size. Still, Eq. (1), together with the experimental release data can be used for determination of an "average" characteristic  $\mu_s$ -value for a given system at a given temperature. This can be done graphically, since with increasing heating time, only the first term in the series becomes effective, giving an exponential release with slope  $-\mu_s$  (and, with the normalization  $F(0) = 1$ , an ordinate intercept of 0.61). The curves in Figs. 2-4 have been fitted to the experimental data by means of Eq. (1).

The  $\mu_s$ -parameter is related to the particle radius ( $r$ ) and the product diffusion coefficient ( $D$ ) in the following way

$$\mu_s = \frac{\pi^2 D}{r^2}. \quad (2)$$

This relation shows the importance of reducing the particle dimensions as much as possible, without causing the mechanism (ii) to become dominant. In principle, knowing  $\mu_s$  and  $r$  for a system,  $D$  can be calculated from Eq. (2). However, due to the uncertainties involved (particularly in  $r$ ), only order of magnitude estimates of  $D$  can be carried out. In cases where  $D$ -values are available from literature, a comparison with experiment may decide the nature of the release-controlling mechanism.

The temperature dependence of  $\mu_s$  is described by the Arrhenius relation:

$$\mu_s = \mu_s^0 e^{-Q/RT}, \quad (3)$$

where  $Q$  is the activation energy for the diffusion process,  $R$  is the gas constant, and  $T$  is the absolute temperature. Note that the relative uncertainty in  $Q$  is much less than in  $D$ , since the uncertainty in  $r$  does not contribute.

A quantity of great importance in characterizing an on-line target system is the release yield  $Y_{\text{obs}}/Y$ , defined as the ratio between the observed yield ( $Y_{\text{obs}}$ ) of a nuclide and the yield ( $Y$ ) that would be obtained if there was no delay in the target system. From the discussion in Ref. 3, it follows that:

$$Y_{\text{obs}}/Y = \frac{3}{\pi} \sqrt{\mu_s/\lambda}, \quad \text{for } \lambda \geq 2\mu_s, \quad (4)$$

where  $\lambda$  is the decay constant for a nuclide being released. This means that the delay properties of specific target materials can be judged as soon as the  $\mu_s$ -values are known.

So far we have neglected the possible influence of mechanism (ii) on the release process. In order to evaluate for which cases such an assumption can be justified, we have to consider the quantities describing the transport of products through a porous solid.

Assuming the transport as occurring through a number of non-intersecting capillaries, one can define an effective diffusion coefficient,  $D_e$ , in the following way<sup>20,21</sup>):

$$D_e = \epsilon^2 \frac{L}{L_e} D_t, \quad (5)$$

where  $\epsilon$  is the porosity,  $L_e/L$  is the ratio of the actual diffusion length to the straight-line distance through the solid, and  $D_t$  corresponds to the diffusion coefficient for diffusion of a product through a cylindrical capillary of radius  $\rho$ . Using Fick's second diffusion equation, one can show that the average time  $\langle t \rangle$  needed for a product to pass through a capillary of length  $L$  is given by<sup>22</sup>)

$$\langle t \rangle = \frac{L^2}{6D_t}. \quad (6)$$



This average time may also be written as<sup>23)</sup>

$$\langle t \rangle = \frac{L^2}{4\rho u} + \frac{L^2\tau}{8\rho^2}, \quad (7)$$

where the first term represents the delay caused by the cosine law of evaporation ( $u$  is the average velocity of the product) and the second is due to the existence of a finite time of surface lingering,  $\tau$ . Surface migration is not included in Eq. (7), since it is believed to be negligible in our cases<sup>23)</sup>. For situations where the first term in Eq. (7) dominates, we find

$$D_t = \frac{2}{3} \rho u, \quad (8)$$

which is the Knudsen diffusion coefficient that usually dominates when physical absorption takes place between product and surface. If the lingering time is high, we get

$$D_t = \frac{4}{3} \frac{\rho^2}{\tau}. \quad (9)$$

The time  $\tau$  is given by the Frankel equation<sup>24)</sup>:

$$\tau = \tau^0 e^{q/kT}, \quad (10)$$

where  $\tau^0$  is a constant of the order of  $10^{-13}$  sec,  $q$  is the surface desorption energy,  $k$  is the Boltzmann constant, and  $T$  the absolute temperature.

Having derived a  $D_e$ -value for a particular system, we can apply the diffusion law in a similar way as described above, now assuming process (ii) to be time controlling. The result is<sup>19)</sup>:

$$F(t) = \frac{8}{\pi^2} \sum_{k=0}^{\infty} \frac{1}{(2k+1)^2} e^{-(2k+1)^2 \mu_p t}, \quad (11)$$

where

$$\mu_p = \frac{\pi^2 D_e}{L_e^2}.$$

For powder systems discussed in this article, at temperatures in the region of 2000°C, the products can be divided into three classes:

- i) Elements of Groups 1A, 8A, and possibly 7A in the periodical system. These products are characterized by Knudsen diffusion in the pore system [Eq. (8)], leading to  $\mu_p \gg \mu_s$ , which means that mechanism (i) will be time-controlling.
- ii) Products of Groups 2A, 6A, 2B, and some other rather volatile elements (Eu, Sm, Yb, In, etc.). In these cases the pore diffusion will be dominated by the lingering time [Eq. (9)], but still  $\mu_p \gg \mu_s$ , which again ensures mechanism (i) to be time-controlling.

iii) Refractory products with very high  $q$ -values, leading to  $\mu_p < \mu_s$ . Such products (Ti, Zr, Hf, etc.) will be strongly delayed in the pore structure of the powder and cannot be produced efficiently from thick powder targets.

Release from a liquid system has been studied in the case of molten  $Ce_3S_4$ . The characteristics of liquid targets are somewhat different from solid targets<sup>5,25</sup>). It is commonly found that the release process can be described by a single exponential function,

$$F(t) = e^{-\mu_\ell t}, \quad (12)$$

where  $\mu_\ell$  is believed to be related to the surface-desorption step. This description also fits the data given in Fig. 6. In this case the release yield is given by<sup>5)</sup>

$$Y_{\text{obs}}/Y = \frac{\mu_\ell}{\mu_\ell + \lambda}. \quad (13)$$

It is interesting to compare Eqs. (4) and (13), which show that the delay properties of solid diffusion-controlled targets depend less strongly on the characteristic parameter  $\mu$  than in the case for those controlled by a single desorption step. This situation is also apparent from Fig. 7.

## 5.2 Sintering effects

It is an empirical observation that when a powder is heated to more than half its melting point, sintering takes place. This process causes the particles to join together, resulting in grain growth and removal of pores. Clearly, the delay properties of powders may be influenced by such effects. In general, the sintering rate is known to depend on the initial particle dimension, self-diffusion coefficient, temperature, and indirectly on vapour pressure<sup>26</sup>). In particular, the first quantity is important, the initial rate being inversely proportional to the cube of the linear dimension of the particle<sup>26</sup>). For this reason, particle sizes below some 1-5  $\mu\text{m}$  are in most cases not suited when a stable powder structure is desirable. Although some models predict grain growth to continue until the theoretical density is reached, it is commonly observed that growth slows down and even stops at larger grain sizes.

To what extent sintering influences the properties of specific target materials can only be determined on the basis of on-line tests, where repeated measurements of the delay properties are performed during prolonged periods of heating. Such tests have been carried out on two systems, i.e. Ta(20) and Nb(20) powder, measuring the delay of Yb and Rb, respectively<sup>3,7</sup>). No changes were found in these two cases. The off-line measurements show, however, that changes must be expected in a number of systems. In general, it appears that ceramic powders are more exposed to sintering than metal powders, possibly because the vapour pressure of

ceramics tend to be higher than for metals, as seen from Table 1. The symptoms of major sintering are:

- No increase in release rates with decreasing particle sizes. (Examples are CeS, VC, UC, and Mo powders. See Figs. 2 and 3 and Table 4.)
- No increase in release rates with increasing temperature. (See results for CeS and BaZrO<sub>3</sub> in Fig. 3 and Table 4.)

Further reference to sintering will be made in the discussion of individual powder materials.

### 5.3 Discussion of individual systems

#### 5.3.1 Hf, Ta, and W

As early as 1965, Andersen et al.<sup>27)</sup> reported a preliminary study of the release of rare-earth elements formed in proton-irradiated Ta-foils, and they pointed out the possibility of using such refractory foils for the production of certain rare earths (RE) at an on-line isotope separator.

Since then comprehensive diffusion studies of RE products in irradiated Hf, Ta, and W foils have been carried out by Beyer<sup>28-30)</sup> and Latuszyński<sup>31)</sup>, based on off-line release measurements. As a general trend, they find not much difference in the diffusion behaviour among rare earths in one defined metal host, while large variations in diffusion coefficients occur for Hf, Ta, and W hosts. Typical values at 2000°C are

$$D_{RE}(Hf) \approx 10^{-7} \text{ cm}^2/\text{sec}, D_{RE}(Ta) \approx 10^{-9} \text{ cm}^2/\text{sec}, D_{RE}(W) \approx 5 \times 10^{-12} \text{ cm}^2/\text{sec} .$$

It may be noted that the trend agrees well with LeClaire's relation given in Section 2. It follows from the discussion in Section 5.1 that with these values for the diffusion coefficients, the diffusion length, for example in Ta, should be less than some 50  $\mu\text{m}$  in order to ensure sufficiently fast release at moderate temperatures ( $\sim 2000^\circ\text{C}$ ). This has been taken into account in our choice of powder particle fractions (see Table 2).

However, as pointed out above, the solid diffusion is only one of the mechanisms responsible for the release process, the other being controlled by the surface desorption energies. It turns out that of the heavy rare earths formed in high yield, only Yb and possibly Tm are sufficiently volatile to escape without serious delay in the pores. These findings agree with what should be expected from desorption measurements performed by Beyer et al.<sup>32)</sup>. By measuring the mean desorption time of carrier-free RE isotopes, they find the desorption energy  $q$  to increase from  $q = 4.2 \text{ eV/atom}$  (Yb) to  $q = 6.4 \text{ eV/atom}$  (Lu), with a general trend which follows the boiling points.

Release measurements of Yb at three different temperatures are shown in Fig. 4. The corresponding Arrhenius plot of the  $\mu_s$ -values (Fig. 5) gives an activation energy of  $105 \pm 10$  kcal/mol, which is close to the  $85 \pm 9$  kcal/mol reported by Beyer et al. for diffusion of Yb in Ta<sup>29)</sup>. Also, diffusion coefficients estimated from Eq. (2) correspond well with those found by Beyer et al., indicating that solid diffusion really is the time-controlling process in the release of Yb. The same situation is found for Yb from Hf, but for Yb from W the release rate is far below that expected from reported D-values<sup>29)</sup>. This is best explained by assuming high surface-desorption energy in the latter case, resulting in substantial pore delay. This explanation is supported by desorption measurements of rare earths from W carried out by Alekseev<sup>33)</sup>. For this reason, W-powder is much less favourable than Hf- and Ta-powders for on-line production of Yb-isotopes.

Expected release-yield curves for on-line production of Yb from different targets are shown in Fig. 7. For Ta(20) [which has been tested in on-line operation<sup>3)</sup>], we have taken the diffusion parameter to be  $\mu_s = 8 \times 10^{-4}$  sec<sup>-1</sup> at 2000°C, as estimated from Fig. 4. For Hf(10) a  $\mu_s$ -value of  $5.7 \times 10^{-3}$  sec<sup>-1</sup> fits the release curve in Fig. 2e, taken at 1900°C. This last value is extrapolated to  $1.2 \times 10^{-2}$  sec<sup>-1</sup> at 2000°C, using the Arrhenius relation and assuming an activation energy of 70 kcal/mol<sup>28)</sup>. Also included in Fig. 7 is a release-yield curve from liquid Lu, since from vapour-pressure considerations<sup>11)</sup> Yb may be expected to be released from such a target. In this case we have assumed  $\mu_\ell = 5.7 \times 10^{-3}$  sec<sup>-1</sup> (delay half-time of 2 min), estimated on the basis of the results from other liquid target systems<sup>5,25)</sup>. We observe a considerable advantage in using Hf-powder for production of Yb-isotopes with half-lives below some 0.5 min. This advantage must, however, be expected to be less pronounced if Hf- and Ta-powders with the same particle size are compared, and it is possible that the difference that still remains may be compensated by raising the temperature of the Ta-target. As seen from Table 1, Hf is limited to about 2000°C, while Ta can be operated well above this temperature.

The optimum value of particle sizes both for Hf and Ta seems to be around 5-10  $\mu$ m. For smaller particles one must expect increased delays coming from surface desorption and sintering effects. Note that the self-diffusion coefficient and vapour pressure (Table 1), which influence the sintering process, are more favourable for Ta than Hf.

### 5.3.2 UC and U(gr)

Escape of fission products, lanthanides and actinides from U-loaded graphite samples, prepared in different ways, has been reported by a number of investigators<sup>6,18,34,35)</sup>.

Cowan and Orth<sup>34)</sup> found rapid release of a number of fission products in the temperature range 1600-2600°C from U-loaded graphite pins. Exceptions were refractory products (Y to Pd) not being released because of high surface-desorption energies. Slow surface desorption may also explain the apparent close relation found between escape fractions and boiling points in the case of lanthanides and actinides<sup>35)</sup>. Of interest is the observation that no U-loss occurred at temperatures below 2050°C, and that the escape rate of products decreased with increasing U-concentration<sup>35)</sup>.

Klapisch et al.<sup>6)</sup> have carried out mass separation of alkali isotopes using targets of UO<sub>2</sub> deposited on thin graphite slabs. The fission recoils are stopped in the graphite and rapid release is obtained at 1500-1600°C. Delay-time components much below 1 sec have been reported.

At OSIRIS, Studsvik, UO<sub>2</sub>-loaded graphite cloth is used for production of short-lived fission products<sup>18)</sup>. Fast release at 1600°C has been observed for fission products, except for the non-volatile elements Y to Pd.

From Figs. 3a,b and Table 4 we notice that most fission products, except the refractory elements, are released from the investigated samples. The release process is presumably controlled by solid diffusion, since available data show that the sequence in escape rate should be Cs > I >> Ba, if the surface desorption energies were controlling<sup>36-38)</sup>. In fact (at a given temperature) the surface lingering time of Ba is many orders of magnitude longer than for Cs<sup>37)</sup>. Also, one should expect, for example, Sn to be released much more slowly than Cs.

Comparing UC(1.3) and UC(20), it turns out that the release rates are rather similar in these two cases. This shows that sintering and grain growth have taken place in the first sample, indicating that no advantage is obtained by using particle sizes below 10-20 μm. In the following we will not distinguish between the two different UC samples, but just refer to the material as UC.

In comparing the production capacity of the different uranium target compositions, two aspects have to be taken into account, i.e. target thickness and delay properties. A target thickness of one interaction length,  $\sim 150 \text{ g/cm}^2$ , corresponds to a filling of UC in the standard 60 cm<sup>3</sup> (20 cm long) target container at ISOLDE<sup>4)</sup>. When going to U(gr), a maximum of 15 g/cm<sup>2</sup> can be obtained in the same geometry, thus giving an order of magnitude lower reaction rate (i.e. true yield, Y). The interesting quantity, however, is the intensity of ion beams at the collector position (observed yield, Y<sub>obs</sub>) which, in general, is lower than the true yield, because of decay losses in the transfer process [see Eq. (4) in Section 5.1].

It is obvious from Figs. 3a,b that U(gr) is a much "faster" target than UC. If we take the release of Cs to represent the performance of the target materials, then we can define a  $\mu_s$ -value for each system

$$\begin{aligned} \mu_s &= 1.5 \times 10^{-3} \text{ sec}^{-1} && \text{for UC at } 2000^\circ\text{C} \\ \mu_s &= 3.3 \times 10^{-3} \text{ sec}^{-1} && \text{for U(gr) at } 1600^\circ\text{C} . \end{aligned}$$

Since a comparison is best made at the same temperature, we assume an activation energy for diffusion of Cs in U(gr) of 70 kcal/mol, as found in on-line experiments<sup>39</sup>). This gives

$$\mu_s = 55 \times 10^{-3} \text{ sec}^{-1} \quad \text{for U(gr) at } 2000^\circ\text{C} .$$

The expected release yields, as a function of product half-life, can now be calculated for both targets at 2000°C (see Fig. 7). We notice that for half-lives below 10 sec the graphite-cloth system is favoured by a factor  $\sim 6$ , thus partially compensating for the 10 times lower target thickness. For half-lives above 1 min no major decay losses are expected in any of the systems. For comparison we also show the expected release yields for Cs-isotopes, released from molten uranium [the problems connected with containing such a corrosive melt over prolonged periods have been discussed in an earlier paper<sup>4</sup>)]. In this case a delay half-time of 30 sec is assumed, a value measured for Cs from molten La<sup>5</sup>). The decay losses of very short-lived isotopes ( $T_{1/2} < 1$  sec) are seen to be substantial.

From the present analysis we conclude that UC powder constitutes a promising target matrix for production of a whole range of fission products. Spallation products like Fr, Rn, At, and Po must also be expected to be released.

For very short-lived isotopes U(gr) may be the best choice, due to its favourable delay properties. The graphite fibres will ensure high long-term stability of the target structure.

### 5.3.3 V, VC and TiC

Interesting reaction products in this region, where the half-lives quickly become short when moving away from stability, are Ar, Cl, and S. The release rates of these products from the three VC samples showed no difference, indicating that sintering and grain growth have taken place, probably influenced by the high vapour pressure of VC at 2300°C. At the more realistic running temperature of 2000°C (not more than 15% linear shrinkage was observed here) good release yields can be expected for isotopes of Ar, Cl, and S.

No escape of products from V metal powder was found. The observed release rates from TiC were well below those from VC (see Figs. 3c,d and Table 4).

### 5.3.4 Nb and Mo

The release of Sr, Rb, and Se has been measured from different Nb and Mo powder samples (Figs. 2a,b,d and Table 4). Due to the absence of convenient isotopes, no measurements of Br and Kr have been performed, but it is expected that also these elements are released.

It soon became apparent that several characteristics of the Nb-powder, for example, fast release of products already at 1650°C, no structural change or target loss even at temperatures above 2000°C, and high density, made this material particularly promising as an ISOLDE target.

A number of on-line investigations were initiated with measurements of yields and delay times of Rb-isotopes from a Nb(20) powder target. Of the results, which are reported in Refs. 3 and 8 and briefly referred to in the Introduction, we mention here that the observed yield of the new isotope  $^{74}\text{Rb}$  (64.9 msec) was found to be 100 times higher than that which was obtained in an early test run with a molten Y-La alloy at 1400°C.

It is interesting to compare the release characteristics of the Mo(20) and Nb(20) powders. Using Se as a representative product, we find

$$\mu_s = 1.15 \times 10^{-3} \text{ sec}^{-1} \quad \text{for Nb(20) at 1650°C .}$$

Extrapolation by means of the Arrhenius relation gives

$$\mu_s = 1.3 \times 10^{-2} \text{ sec}^{-1} \quad \text{for Nb(20) at 2000°C ,}$$

taking the activation energy to be the same as for Rb, 60 kcal/mol<sup>3)</sup>. This should be compared to the observed value:

$$\mu_s = 7.7 \times 10^{-4} \text{ sec}^{-1} \quad \text{for Mo(20) at 2000°C .}$$

The corresponding release yield curves are shown in Fig. 7, from which the gain in using Nb can be evaluated.

The ratio between the diffusion parameters ( $\sim 20$  in favour of Nb) is significantly higher than the corresponding ratio between the self-diffusion coefficients ( $\sim 4$ , see Table 1). This may indicate that the diffusion mechanism of products in the Nb host is influenced by interstitial components, which are known to result in enhanced diffusion<sup>16)</sup>.

We notice from Fig. 2d that the release of Se from Mo(2) is slower than from Mo(20), presumably as a result of sintering effects. Thus, the optimum particle size seems to lie around 10-20  $\mu\text{m}$  for Mo, and probably similarly for Nb.

#### 5.3.5 BaZrO<sub>3</sub>, LaB<sub>6</sub>, CeB<sub>6</sub>, CeS<sub>2</sub>, and Ce<sub>3</sub>S<sub>4</sub>

Molten La for production of Cs isotopes has been in use at ISOLDE for a number of years<sup>4)</sup>. Release of Xe and I from molten La has been observed in off-line experiments, while Te and Sb are found to be retained in the melt<sup>4)</sup>.

Preliminary on-line tests at ISOLDE of a ceramic CeO<sub>2</sub> target have been reported by Hansen et al.<sup>7)</sup>. No delay measurements were performed, but reasonable

yields of the elements Cs, Xe, I, Te, and Sb were observed. A limitation had to be put on the target temperature, however, as it was found that CeO<sub>2</sub> begins to react with the Ta container already at 1550°C.

On this basis, we decided to investigate a series of refractory compounds to search for alternative targets with better delay and stability properties.

Of those tested, BaZrO<sub>3</sub> and CeS represent the best cases (see Figs. 3e,f and Table 4), although the characteristics are not as favourable as for some of the metal powders discussed above. However, at a running temperature of maximum 1900°C, using Ta containers, they should offer good alternatives to CeO<sub>2</sub> for production of Te and Sb. The elements Cs, Xe, and possibly I are still most efficiently produced from molten La.

An interesting possibility for production of Te is offered by the molten Ce<sub>3</sub>S<sub>4</sub> at 1900-2000°C (see Fig. 6). The delay half-time of ~ 40 sec ensures good release yields of Te isotopes with half-lives in the second range or above. The ~ 20 sec delay half-time for Cs is about the same as found for Cs from molten La<sup>5)</sup>.

An interesting ceramic system, although so far not tested, is cerium carbide (CeC). This compound has a reported melting point of 2500°C and a vapour pressure at 2000°C of ~ 10<sup>-4</sup> Torr<sup>40)</sup>, which bring the physical properties very close to those of UC. Thus, by analogy with the corresponding U-targets (see Figs. 3a,b and text above), Ce-impregnated graphite cloth or pure CeC-powder may be expected to show favourable properties as targets in the Cs-Te region.

## 6. CONCLUDING REMARKS

The present investigations have brought out that a number of refractory materials, prepared in a powdery form, represent efficient target systems for on-line production of a range of elements. A summary of the most promising powders and some 30 different elements expected to be separated at ISOLDE is given in Fig. 8.

Finally, we would like to stress that on-line measurements of release rates may differ somewhat from those measured off line, owing to the influence of radiation effects. It is known that when a crystal is subjected to ionizing radiation, additional vacancies and interstitials are created in concentrations which may far exceed those produced thermally<sup>41)</sup>. This means that enhanced diffusion can occur during irradiation, clearly seen, for example, in the on-line study of Rb from hot Nb-powder<sup>3)</sup>, where the diffusion parameter ( $\mu_s$ ) increased by a factor of approximately five compared to the value measured off line. For chemical-compound targets the situation may be somewhat different, since the chemical damage induced by nuclear events (resulting in decomposition of the compound) can affect the



porous structure of the target material. Although thermal annealing processes may repair the chemical damage, it is uncertain how sintering and shrinkage properties will be affected during this process. On-line experiments<sup>39)</sup>, which are in progress, will give the answer to these problems.

#### Acknowledgements

We are indebted to O.C. Jonsson for his contribution to the choice and testing of  $\text{BaZrO}_3$  as a prospective target material.

Two of us (I.R.H. and L.W.) would like to thank the Norwegian Research Council for Science and the Humanities for financial support.

REFERENCES

- 1) A. Kjelberg and G. Rudstam (eds.), CERN 70-3 (1970).
- 2) S. Sundell, P.G. Hansen, B. Jonson, E. Kugler, H.L. Ravn and L. Westgaard, Proc. 8th Internat. EMIS Conf. on Low-energy Ion Accelerators and Mass Separators, Skövde, 1973 (eds. G. Andersson and G. Holmén) (Chalmers Univ. of Technology and Univ. of Gothenburg, Gothenburg, Sweden, 1973), p. 335.
- 3) H.L. Ravn, L.C. Carraz, J. Denimal, E. Kugler, M. Skarestad, S. Sundell and L. Westgaard, Nuclear Instrum. Methods 139 (1976) 267.
- 4) H.L. Ravn, S. Sundell and L. Westgaard, Nuclear Instrum. Methods 123 (1975) 131.
- 5) H.L. Ravn, S. Sundell, E. Roeckl and L. Westgaard, J. Inorg. Nuclear Chem. 37 (1975) 383.
- 6) R. Klapisch, J. Chaumont, C. Philippe, I. Amarel, R. Fergerau, M. Salome and R. Bernas, Nuclear Instrum. Methods 53 (1967) 216.
- 7) F. Hansen, A. Lindahl, O.B. Nielsen and G. Sidenius, Proc. 8th Internat. EMIS Conf. on Low-energy Ion Accelerators and Mass Separators, Skövde, 1973 (eds. G. Andersson and G. Holmén) (Chalmers Univ. of Technology and Univ. of Gothenburg, Gothenburg, Sweden, 1973), p. 426.
- 8) J.M. D'Auria, L.C. Carraz, P.G. Hansen, B. Jonson, S. Mattsson, H.L. Ravn, M. Skarestad, L. Westgaard and The ISOLDE Collaboration, Phys. Letters 66B (1977) 233.
- 9) E.K. Storms, The refractory carbides (Academic Press, New York, 1967).
- 10) G.L. DePoorter and T.C. Wallace, *in* Advances in high temperature chemistry, (ed. L.E. Eyring); (Academic Press, New York, 1971), p. 107.
- 11) R. Hultgren, P.D. Desai, D.T. Hawkins, M. Gleiser, K.K. Kelley and D.D. Wagman, Selected values of the thermodynamic properties of the elements (Amer. Soc. for Metals, Ohio, 1973).
- 12) J.M. Lafferty, J. Appl. Phys. 22 (1951) 229.
- 13) E.D. Eastman, L. Brewer, L.A. Bromley, P.W. Gilles and N.L. Lofgren, J. Amer. Chem. Soc. 72 (1950) 2248.
- 14) Landholt-Börnstein, Zahlenwerte und Funktionen, Vol. 2, Part 5b (Springer Verlag, Berlin, 1968).
- 15) R.C. Weast, Handbook of chemistry and physics, 55th edn. (The Chemical Rubber Co., Cleveland, Ohio, 1975).
- 16) A.S. Norwick and I.J. Burton, Diffusion in solids: recent developments (Academic Press, London, 1975).
- 17) A.D. LeClaire, Progr. Metal Phys. 306 (1949) 1.
- 18) Ch. Andersson, B. Grapengiesser and G. Rudstam, The Swedish Research Councils' Laboratory, Studsvik Research Report LF-45 (1973).
- 19) J. Crank, The mathematics of diffusion (Clarendon Press, Oxford, 1957).

- 20) A. Wheeler, *Catalysis* 2 (1955) 105.
- 21) P.B. Weisz and A.B. Schwartz, *J. Catal.* 1 (1962) 399.
- 22) G.R. Youngquist, *Industr. Engng. Chem.* 62 (1970) 53.
- 23) J.H. DeBoer, *The dynamical character of adsorption* (Clarendon Press, Oxford, 1968), p. 29.
- 24) *Ibid*, p. 232.
- 25) E. Hagebø, A. Kjelberg, P. Patzelt, G. Rudstam and S. Sundell, CERN 70-3 (1970), p. 93.
- 26) J.E. Burke, *Chemical and mechanical behaviour of inorganic materials* (eds. A.W. Searcy, D.V. Ragone and U. Colombo) (Wiley, New York, 1970), p. 413.
- 27) M.L. Andersen, O.B. Nielsen and B. Scharff, *Nuclear Instrum. Methods* 8 (1965) 303.
- 28) G.J. Beyer and A.F. Novgorodov, Report ZFK 303 (Zentralinstitut für Kernforschung, Rossendorf, Dresden, 1976).
- 29) G.J. Beyer and A.F. Novgorodov, Report ZFK 310 (Zentralinstitut für Kernforschung, Rossendorf, Dresden, 1976).
- 30) G.J. Beyer, A.F. Novgorodov and W.D. Fromm, Report ZFK 309 (Zentralinstitut für Kernforschung, Rossendorf, Dresden, 1976).
- 31) A. Latuszyński, K. Zuber, J. Zuber, A. Potempa and W. Żuk, *Nuclear Instrum. Methods* 120 (1974) 321.
- 32) G.J. Beyer and A.F. Novgorodov, Report ZFK 305 (Zentralinstitut für Kernforschung, Rossendorf, Dresden, 1976).
- 33) N.I. Alekseev, *Soviet Phys. Tech. Phys. (USA)* 12 (1968) 1639.
- 34) G. Cowan and C.J. Orth, *Proc. 2nd Internat. Conf. on Peaceful Uses of Atomic Energy, Geneva, 1958* (United Nations, Geneva, 1959), Vol. 7, p. 328.
- 35) C.J. Orth, *Nuclear Sci. Engng.* 9 (1961) 417.
- 36) M.D. Scheer, R. Klein and J.D. McKinley, *Adsorption and desorption phenomena* (ed. F. Ricca) (Academic Press, New York, 1972), p. 169.
- 37) M.D. Scheer and J. Fine, *J. Chem. Phys.* 38 (1963) 307.
- 38) M.D. Scheer and J. Fine, *J. Chem. Phys.* 37 (1962) 107.
- 39) L.C. Carraz, M. Skarestad, S. Sundell, H.L. Ravn and L. Westgaard, *High-temperature carbide targets for fast on-line isotope separation of alkali and noble gas elements, to be published.*
- 40) Yu.B. Paderno, V.S. Fomenko, I.A. Podchernyaeva and G.N. Makarenko, *Soviet Phys. Tech. Phys. (USA)* 10 (1966) 1434.
- 41) G. Dearnaley, J.H. Freeman, R.S. Nelson and J. Stephen, *Ion implantation* (North-Holland, Amsterdam, 1973).

Table 1

Physical and thermodynamic properties of investigated materials

Chemical composition	Melting point (°C)	Vapour pressure at 2000°C (Torr)	Crystal density (g/cm <sup>3</sup> )	D <sub>self</sub> × 10 <sup>12</sup> at 2000°C b) (cm <sup>2</sup> /sec)	Maximum temperature c) (°C)	Crucible material	References d)
W	3400	1.2 × 10 <sup>-8</sup>	19.3	1.2	> 2300	Ta	11, 11, 15, 14
Ta	2980	1.7 × 10 <sup>-7</sup>	16.6	50	> 2300	Ta	11, 11, 15, 14
Hf	2220	3.2 × 10 <sup>-4</sup>	13.3		2100	Ta	11, 11, 15
Mo	2620	1.4 × 10 <sup>-4</sup>	10.2	200	2300	Ta	11, 11, 15, 14
Nb	2467	1.1 × 10 <sup>-5</sup>	8.6	800	2300	Ta	11, 11, 15, 14
V	1900	7.5 × 10 <sup>-3</sup> e)	6.1	11000 e)	1700	Ta	11, 11, 15, 14
UC	2500	7.6 × 10 <sup>-6</sup>	11.2	30 (U)	2300	Graphite	9, 9, 15, 10
VC	2700	7.6 × 10 <sup>-4</sup>	5.7	8 (V)	2000	Graphite	9, 9, 15, 10
TiC	2800	1.5 × 10 <sup>-4</sup>	4.9	0.4 (Ti)	2000	Graphite	9, 9, 15, 10
CeS	2450	10 <sup>-3</sup>	5.9		1900	Ta	13, 13, 13
Ce <sub>3</sub> S <sub>4</sub>	2000	10 <sup>-3</sup>	5.3		1900	Ta	13, 13, 13
LaB <sub>6</sub>	2210	1.5 × 10 <sup>-3</sup>	5.2		1900	Graphite	12, 12, 12
CeB <sub>6</sub>	2190	10 <sup>-3</sup>	5.2		1900	Graphite	12, 12, 12
BaZrO <sub>3</sub>	2500 g)	10 <sup>-4</sup> e,f)	5.0 g)		1900	Ta	12, 12, 12

a) About 50-70% porosity of non-sintered powder material can be assumed.

b) The column gives the self-diffusion coefficient in refractory materials.

c) The temperatures refer to the maximum values at which the powders can be operated at ISOLDE. The limit for safe technical operation lies currently at 2300°C.

d) References for the data in columns 2, 3, 4, 5 (in that order).

e) The value given corresponds to a temperature of 1800°C.

f) Vapour pressure estimated from measured evaporation losses.

g) Data supplied by manufacturer.

Table 2

Mechanical specification of materials investigated

Material	Particle-size distribution ( $\mu\text{m}$ )	Average dimensiona) ( $\mu\text{m}$ )	Symbol used in text	Supplier
W	5-20 b)	10	W(10)	H.C. Stark, Berlin
	10-30 b)	20	W(20)	H.C. Stark, Berlin
Ta	1-44 b)	6	Ta(6)	Norton Metals Division, Lausanne
	1-44 b)	10	Ta(10)	Norton Metals Division, Lausanne
	1-75 b)	20	Ta(20)	Norton Metals Division, Lausanne
Hf	20-40 c)	30	Hf(30)	Goodfellow Metals Ltd., Cambridge
	1-20 c)	10	Hf(10)	Goodfellow Metals Ltd., Cambridge
Mo		2	Mo(2)	Goodfellow Metals Ltd., Cambridge
	15-30 b)	20	Mo(20)	H.C. Stark, Berlin
	30-50 b)	40	Mo(40)	H.C. Stark, Berlin
Nb	1-40 b)	20	Nb(20)	Goodfellow Metals Ltd., Cambridge
V	45-150 b)	100	V(100)	Goodfellow Metals Ltd., Cambridge
UC	0.7-15 b)	1.3	UC(1.3)	Lab. Chim. Nucl., Grenoble
UC+UC <sub>2</sub>	1-50 b)	20	UC(20)	Ventron Corp., Karlsruhe
VC	1-50 b)	10	VC(10)	Ventron Corp., Karlsruhe
	1-10 c)	5	VC(5)	Ventron Corp., Karlsruhe
	10-25 c)	15	VC(15)	Ventron Corp., Karlsruhe
TiC	1-50 b)	10	TiC(10)	Ventron Corp., Karlsruhe
CeS	1-25 c)	10	CeS(10)	ICN Pharmaceuticals Inc., New York
	25-40 c)	30	CeS(30)	ICN Pharmaceuticals Inc., New York

Table 2 (contd.)

Material	Particle-size distribution ( $\mu\text{m}$ )	Average dimension <sup>a</sup> ( $\mu\text{m}$ )	Symbol used in text	Supplier
CeB <sub>6</sub>	1-40 b)	10	CeB <sub>6</sub> (10)	Ventron Corp., Karlsruhe
LaB <sub>6</sub>	1-40 b)	10	LaB <sub>6</sub> (10)	Ventron Corp., Karlsruhe
BaZrO <sub>3</sub>	tested in a molten form	1.2	BaZrO <sub>3</sub> (1.3)	Ventron Corp., Karlsruhe
Ce <sub>3</sub> S <sub>4</sub>			Ce <sub>3</sub> S <sub>4</sub> (liq)	Ventron Corp., Karlsruhe
Uranium-loaded graphite cloth. (The graphite cloth, consisting of 20 $\mu\text{m}$ graphite fibres, Grade WCA, was impregnated in our laboratory.)				
			U(gr)	Union Carbide, Geneva

a) This column gives the average particle diameter, based on manufacturer-supplied data [Ta(6), Ta(10), Ta(20), Mo(2), UC(1.3), BaZrO<sub>3</sub>(1.2)], or our own measurements using a number of fine-meshed sieves.

b) Particle-size distribution supplied by manufacturer.

c) Particle fractions separated by use of sieves.

Table 3

Properties of nuclides used in the release measurements<sup>a)</sup>

Host	Nuclide	Half-life	γ-energy (keV)	Host	Nuclide	Half-life	γ-energy (keV)
Mo, Nb	<sup>82</sup> Sr	25 d	777	UC, U(gr)	<sup>140</sup> La	40 h	1596
	<sup>84</sup> Rb	33 d	882		<sup>140</sup> Ba	12 d	537
	<sup>83</sup> Rb	83 d	520,529		<sup>136</sup> Cs	13 d	819,1047
	<sup>75</sup> Se	120 d	136		<sup>131</sup> I	8 d	365
W, Ta, Hf	<sup>169</sup> Yb	31 d	177,198		<sup>132</sup> Te	78 h	228
	<sup>167</sup> Tm	9 d	208		<sup>126</sup> Sb	12.4 d	666,695
CeB <sub>6</sub> , CeS, Ce <sub>3</sub> S <sub>4</sub> , LaB <sub>6</sub> , BaZrO <sub>3</sub>	<sup>140</sup> La	40 h	1596		<sup>122</sup> Sb	2.7 d	564
	<sup>128</sup> Ba	2.4 d	273		<sup>120</sup> Sb	5.7 d	1022,1171
	<sup>131</sup> Ba	9.7 d	124,496		<sup>117m</sup> Sn	14 d	159
	<sup>129</sup> Cs	32 h	372		<sup>115m</sup> In	4.5 h	336
	<sup>132</sup> Cs	6.5 d	668		<sup>115</sup> Cd	53 h	528
	<sup>125</sup> Xe	17 h	188		<sup>105</sup> Rh	35 h	319
	<sup>127</sup> Xe	36 d	172,203		<sup>103</sup> Ru	39 d	497
	<sup>123</sup> I	13 h	159		<sup>99m</sup> Tc	6 h	141
	<sup>124</sup> I	4 d	603	<sup>99</sup> Mo	66 h	181,740	
	<sup>119</sup> Te	16 h	644	<sup>95</sup> Nb	35 d	766	
	<sup>121</sup> Te	17 d	573	<sup>95</sup> Zr	64 d	757,724	
	<sup>120</sup> Sb	5.8 d	1172	TiC, VC, V	<sup>47</sup> Ca	4.5 d	1297
	<sup>113</sup> Sn	115 d	255		<sup>43</sup> K	22 h	373
			<sup>41</sup> Ar		1.8 h	1294	
				<sup>39</sup> Cl	56 min	1267	
				<sup>38</sup> S	2.8 h	1942	

a) Data from C.M. Lederer, J.M. Hollander and I. Perlman, Table of isotopes, 6th edn. (Wiley, New York, 1967).

Table 4

Release of reaction products from different powders

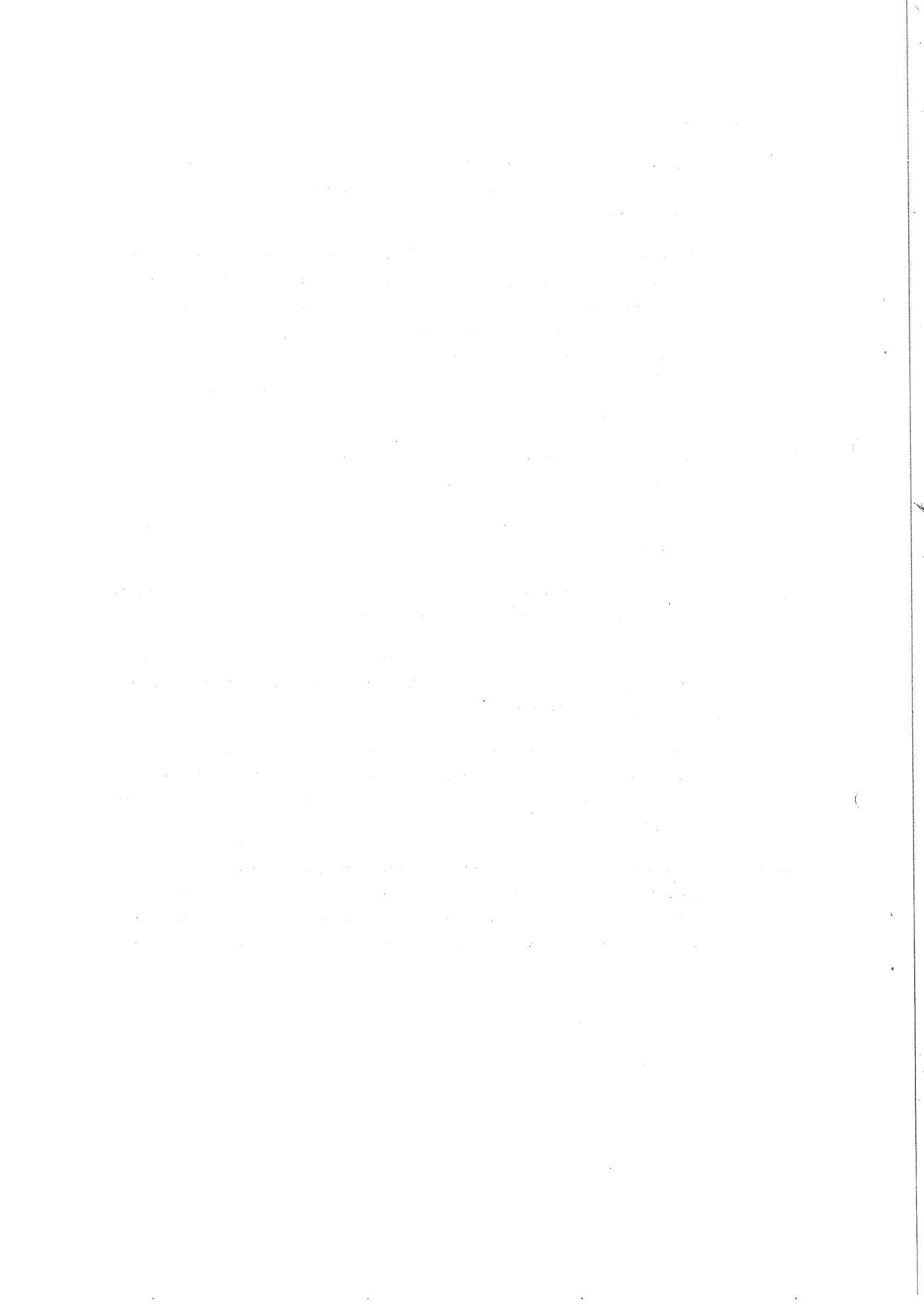
Powder	Product element	Heating time (min)	Temperature (°C)	Fractional activity <sup>a)</sup>
Nb(20)	Sr,Rb	5	1850	0.20
Hf(30)	Tm	3	1900	0.42
Hf(10)	Tm	3	1900	0.17
Ta(6)	Tm	6	2000	0.23
Ta(10)	Tm	6	2000	0.50
Ta(20)	Tm	6	2000	0.50
CeB <sub>6</sub> (10)	Ba	3	2060	0.90
	Cs,Xe	3	2060	0.70
	I,Te	3	2060	0.40
LaB <sub>6</sub> (10)	Ba,Cs,Xe,I,Te	3	2000	No release
V(100)	K,Ar	3	1800	No release
VC(5),VC(10)	Ca,K,Ar	3 and 8	2300	Same as for VC(15) (Fig. 3c)
UC(1.3)	Ba,Cs,I,Te,Sn	5 and 15	2000	Same as for UC(20) (Fig. 3b)
CeS(10)	Ba,Cs,Xe,I,Te	3 and 10	2000	Same as for CeS(30) (Fig. 3e)
CeS(30)	Cs	3	1850	Same as at 2000°C (Fig. 3e)
BaZrO <sub>3</sub>	Cs,I,Te,Sb	5	1900	Same as at 1800°C (Fig. 3f)

a) Quantity defined in Section 4.2.



Figure captions

- Fig. 1 : The sample contained in a tantalum boat is being placed in the tubular oven, which is suspended inside the chamber of a usual vacuum coating unit.
- Fig. 2 : Release of reaction products from irradiated refractory metal powders. The points represent measured fractional activities (defined as the ratio between the activity of a given nuclide in a sample after a heating period and the activity before any heating treatment) as a function of sample heating time.  
The curves have been fitted to the experimental points according to Eq. (1) in the text.
- Fig. 3 : Release of reaction products from irradiated powders of refractory compounds. See capture in Fig. 2.
- Fig. 4 : Release of Yb from irradiated Ta(20) at three different temperatures. See capture in Fig. 2.
- Fig. 5 : The diffusion parameter  $\mu_s$  for release of Yb from Ta(20) as a function of the inverse of the absolute temperature.
- Fig. 6 : Release of reaction products from molten  $Ce_3S_4$ . The points represent measured fractional activities. The curves have been drawn according to Eq. (12) in the text.
- Fig. 7 : Calculated release yields  $Y_{obs}/Y$  (ratio of observed yield and yield that would be observed if no decay losses occurred) for different target systems as a function of the half-life of the nuclear reaction product.
- Fig. 8 : Periodical system of the elements, indicating those powder (or fibre) targets which are either in present use or foreseen to become operative in the near future for on-line experiments at ISOLDE, together with the product elements expected to be separated from these targets.



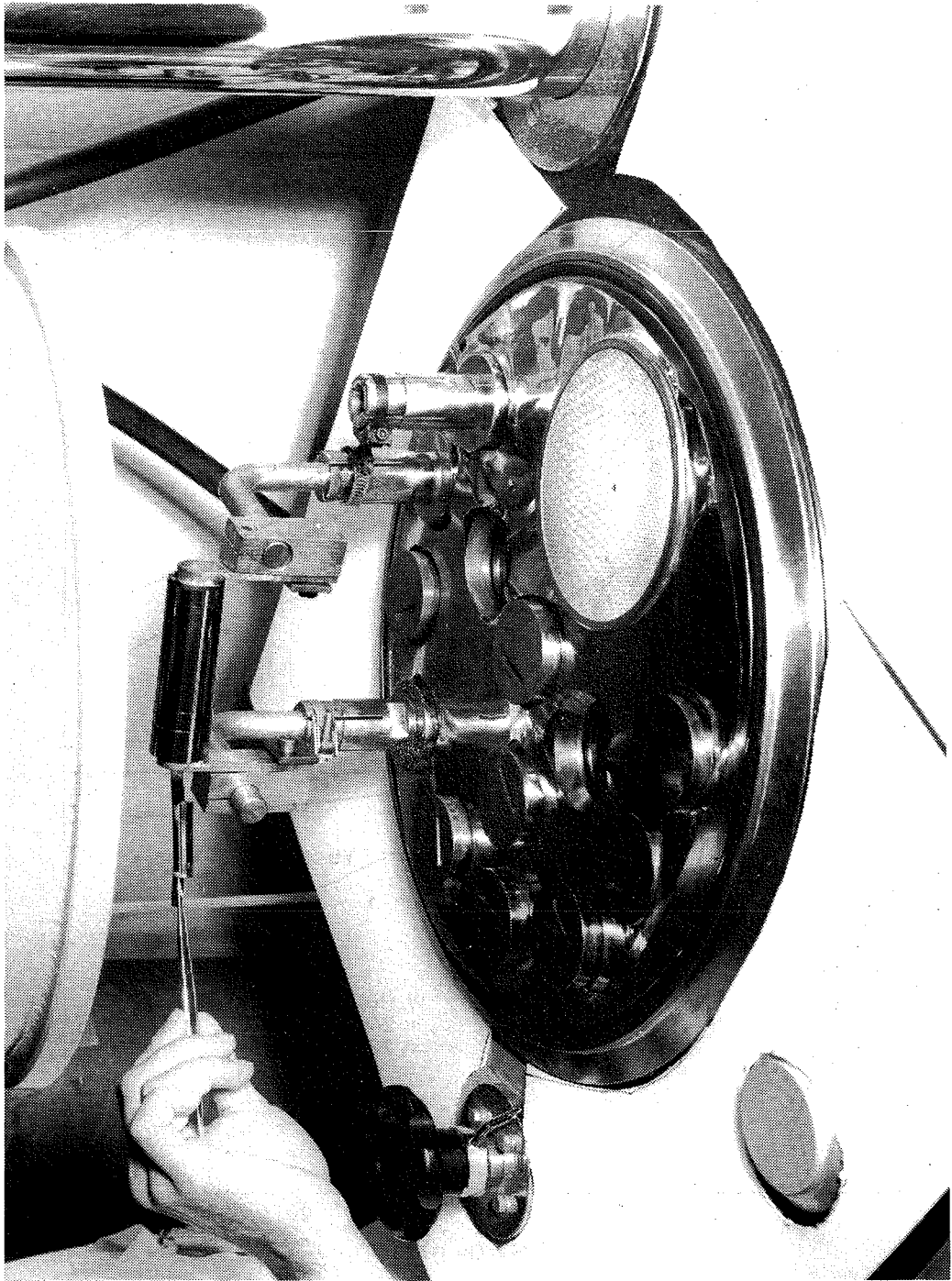


Fig. 1

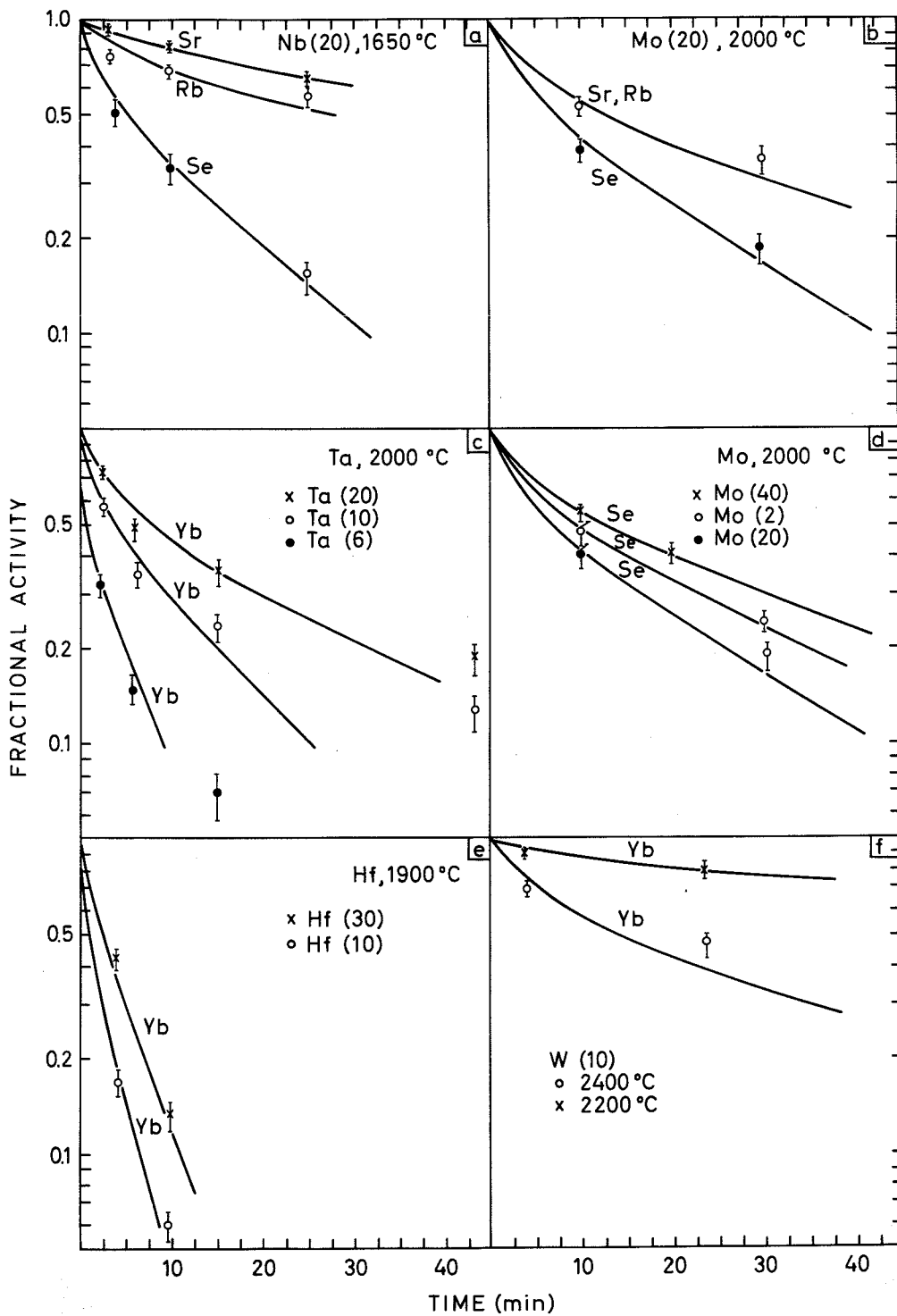


Fig. 2

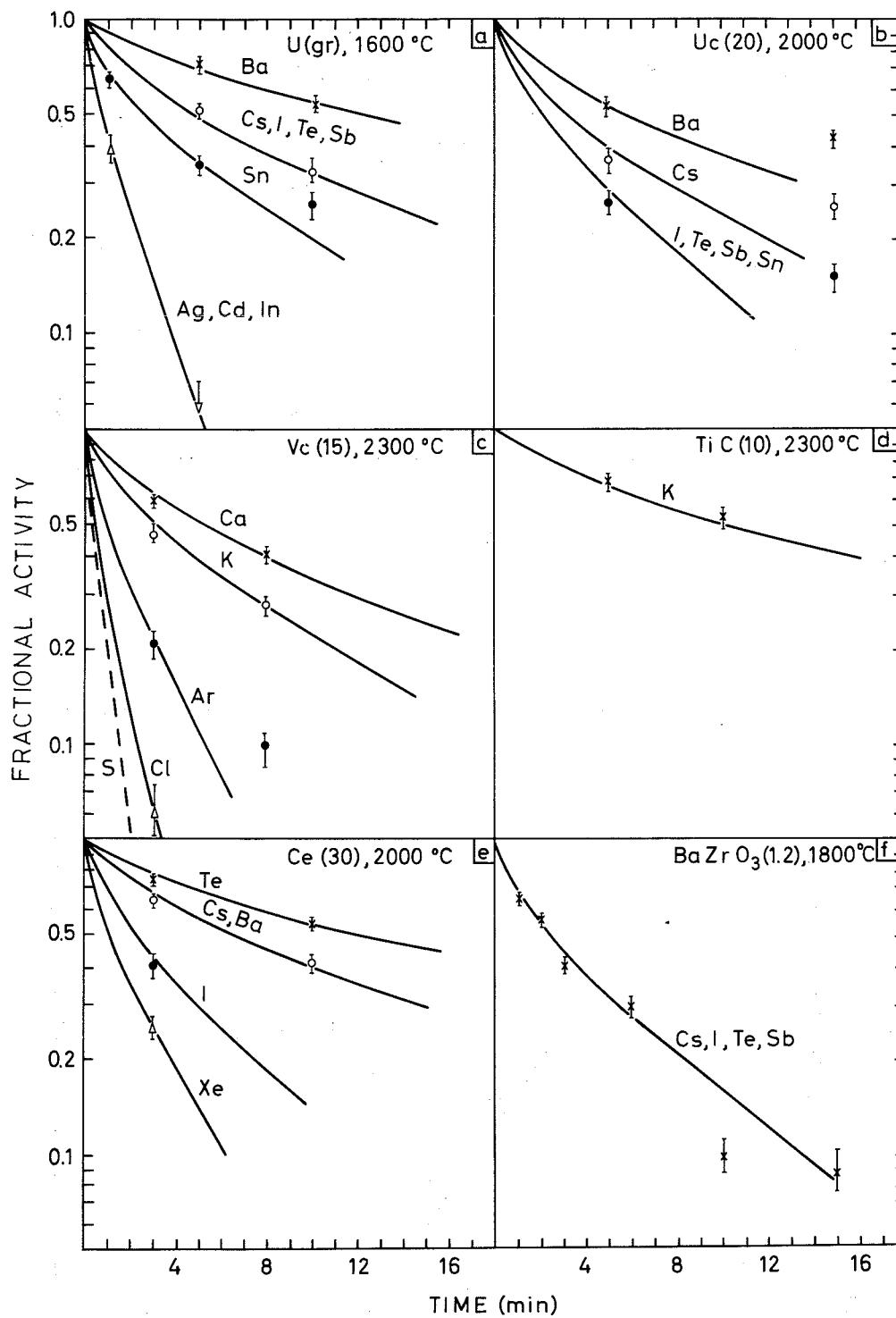


Fig. 3

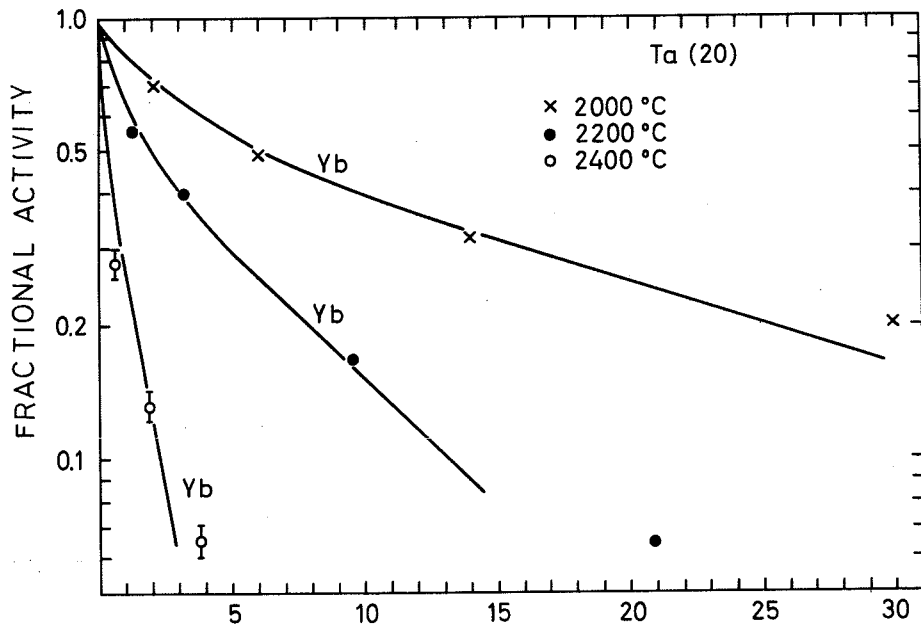


Fig. 4

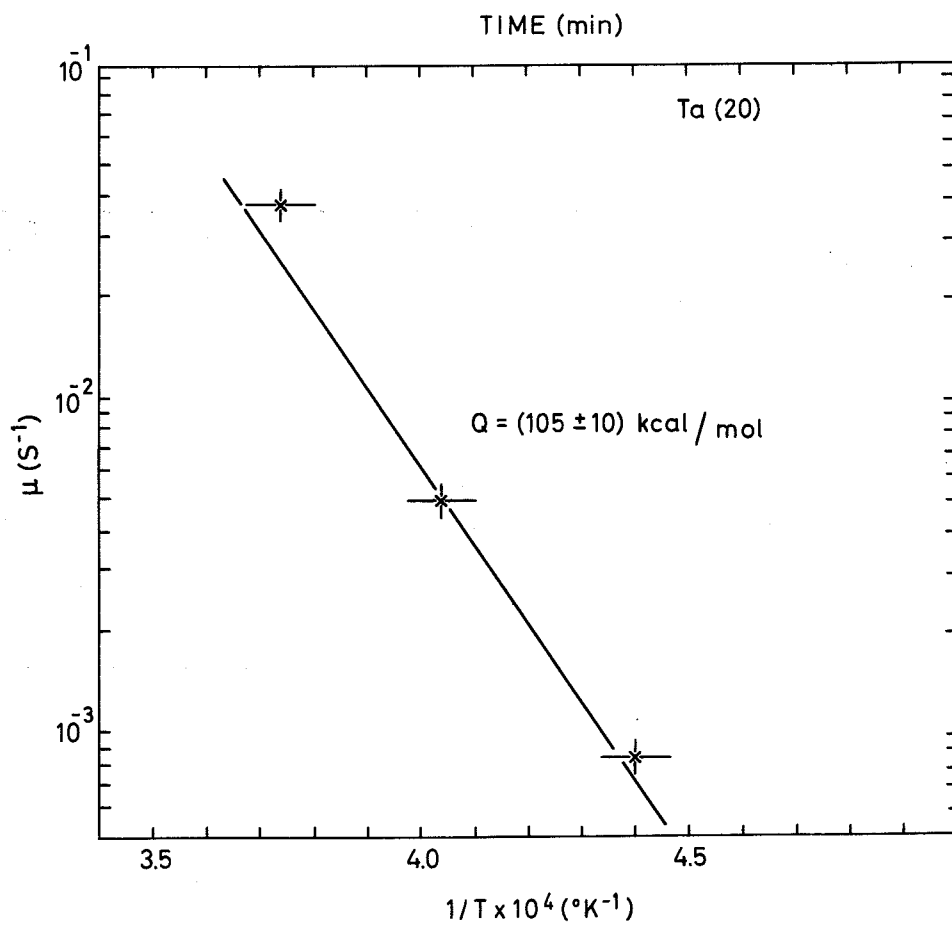


Fig. 5

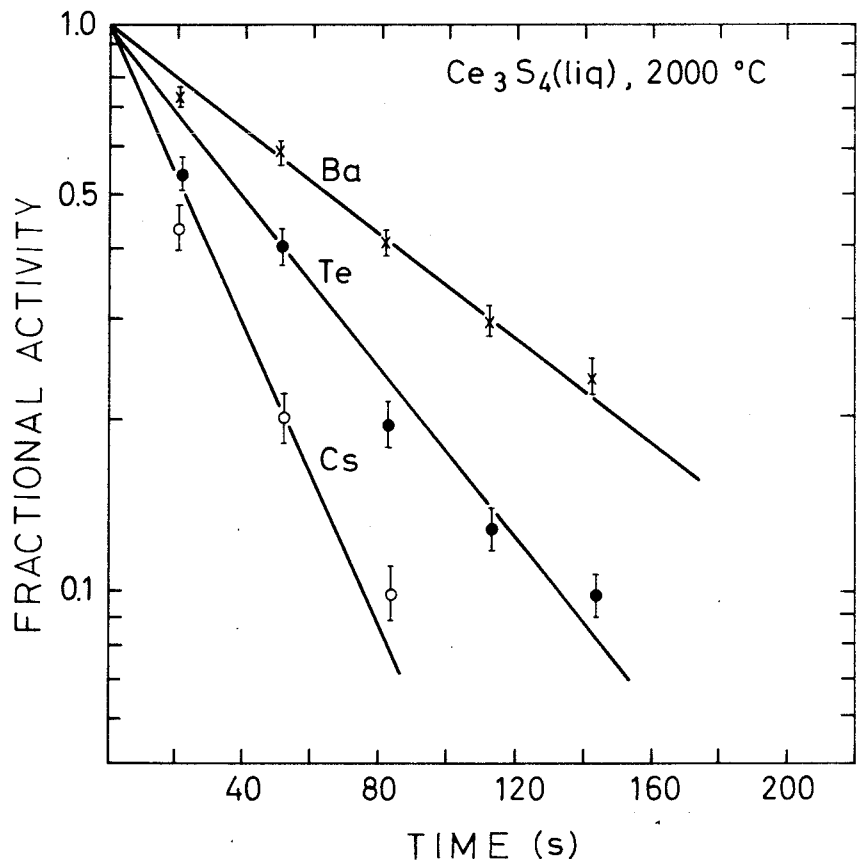


Fig. 6

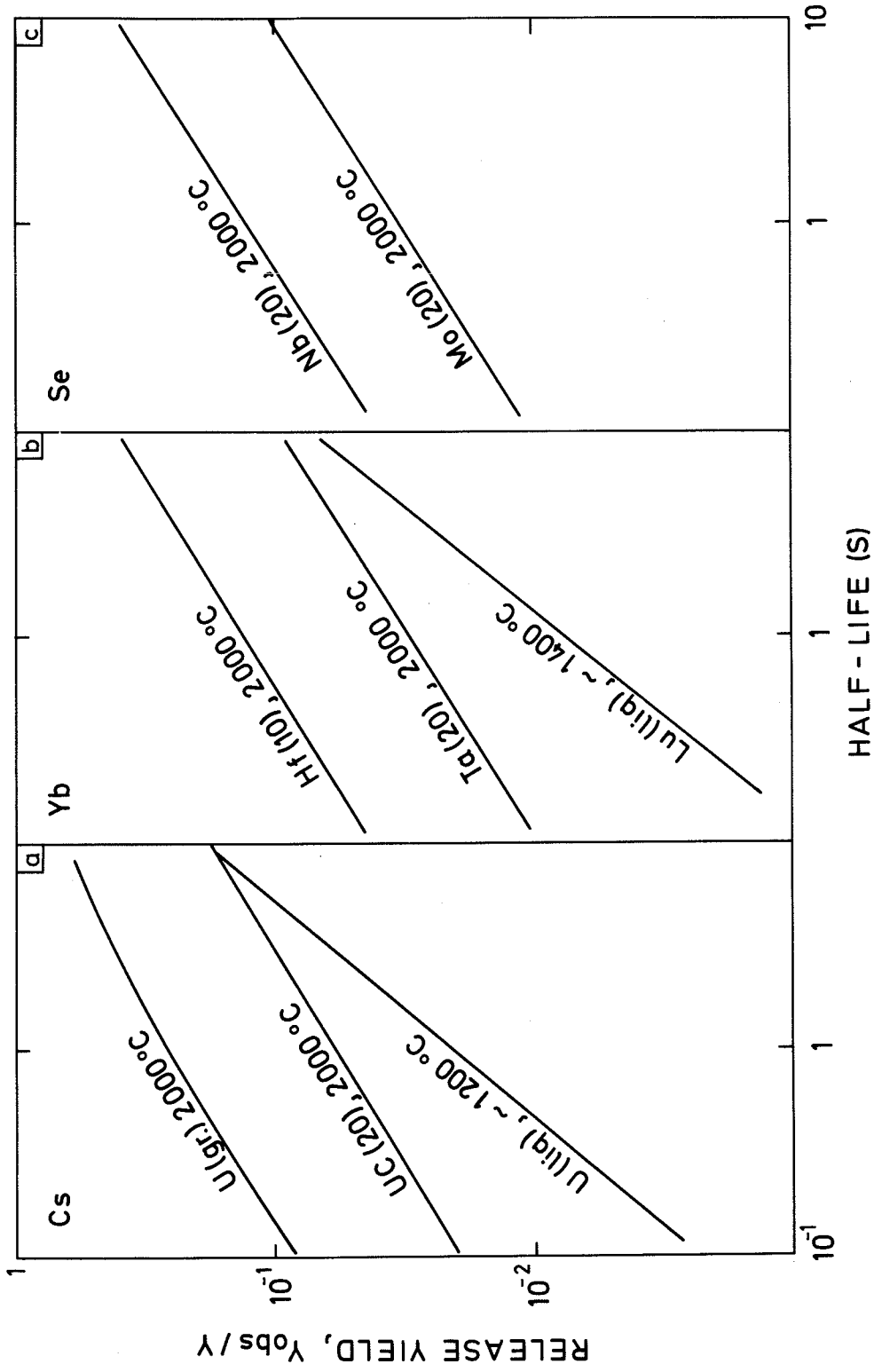



Fig. 7



IA	H																	VIIIA	He						
IIA	Li	Be																	IIIA	B	C	N	O	F	Ne
	Na	Mg											IIIB	Al	Si	P	S	Cl	Ar						
	K	Ca	Sc	Ti	V	Cr	Mn	Fe	Co	Ni	Cu	Zn	Ga	Ge	As	Se	Br	Kr							
	Rb	Sr	Y	Zr	Nb	Mo	Tc	Ru	Rh	Pd	Ag	Cd	In	Sn	Sb	Te	I	Xe							
	Cs	Ba	La	Hf	Ta	W	Re	Os	Ir	Pt	Au	Hg	Tl	Pb	Bi	Po	At	Rn							
	Fr	Ra	Ac																						
LANTHANIDES	Ce	Pr	Nd	Pm	Sm	Eu	Gd	Tb	Dy	Ho	Er	Tm	Yb	Lu											
ACTINIDES	Th	Pa	U	Np	Pu	Am	Cm	Bk	Cf	Es	Fm	Md	No	Lr											

 Powder target

 Product element

Fig. 8

